ACS Catalysis

pubs.acs.org/acscatalysis

Letter

A Molecular Iron-Based System for Divergent Bond Activation: Controlling the Reactivity of Aldehydes

Basujit Chatterjee,[#] Soumyashree Jena,[#] Vishal Chugh, Thomas Weyhermüller, and Christophe Werlé*

Cite This: *ACS Catal.* 2021, 11, 7176–7185

Read Online

ACCESS | Metrics & More | Article Recommendations | Supporting Information

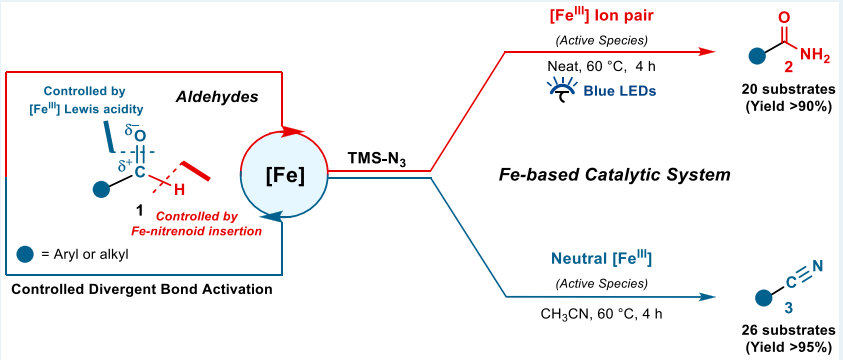

ABSTRACT: The direct synthesis of amides and nitriles from readily available aldehyde precursors provides access to functional groups of major synthetic utility. To date, most reliable catalytic methods have typically been optimized to supply one product exclusively. Herein, we describe an approach centered on an operationally simple iron-based system that, depending on the reaction conditions, selectively addresses either the C═O or C−H bond of aldehydes. This way, two divergent reaction pathways can be opened to furnish both products in high yields and selectivities under mild reaction conditions. The catalyst system takes advantage of iron's dual reactivity capable of acting as (1) a Lewis acid and (2) a nitrene transfer platform to govern the aldehyde building block. The present transformation offers a rare control over the selectivity on the basis of the iron system's ionic nature. This approach expands the repertoire of protocols for amide and nitrile synthesis and shows that fine adjustments of the catalyst system's molecular environment can supply control over bond activation processes, thus providing easy access to various products from primary building blocks.

KEYWORDS: *molecular system, bond activation, homogeneous catalysis, divergent reactivity, ion pair, aldehyde, amide and nitrile synthesis*

INTRODUCTION

Nature's biological instruments can operate countless parallel processes with incomparable levels of efficiency.[1] This chemical machinery demonstrates that, despite a complex reaction medium with numerous prospective reaction partners, precise control over the bond activation processes and catalytic sequences can be achieved, furnishing products in high selectivity. In contrast, catalytic protocols are traditionally designed to convert substrates, preferably or even exclusively, into a single product.[2] Alternatively, one might envisage the catalyst as a system whose activity can be comprehensively controlled by fine adjustments of reaction conditions to convey distinct product platforms.[3] The development of such dynamic catalytic systems supports the concept of molecularly controlled catalysis.[4]

In this approach, understanding and designing catalytic systems in their full complexity are key. This may lead to responsive or adaptive catalysts for which precise control and regulation of the catalytic activity are possible. Accordingly, responsive systems may modulate their activity based on external stimuli;[5] in contrast, adaptive catalysts may change their chemical reactivity in response to the reaction conditions, and components, to generate different products.[3e] Here, reaction parameters are combined rather than isolated, and their function and interactions are studied within the entire system. This way, new synergies can be identified, ultimately creating new properties present in the system, not in its parts. Thus, the catalyst may appear to be self-adjusting, controlled and regulated by a specific environment for a particular set of

Received: February 15, 2021
Revised: April 23, 2021
Published: June 4, 2021

https://doi.org/10.1021/acscatal.1c00733
ACS Catal. 2021, 11, 7176–7185

Scheme 1. Development of an Iron-Based System for Divergent Bond Activation in Aldehydes

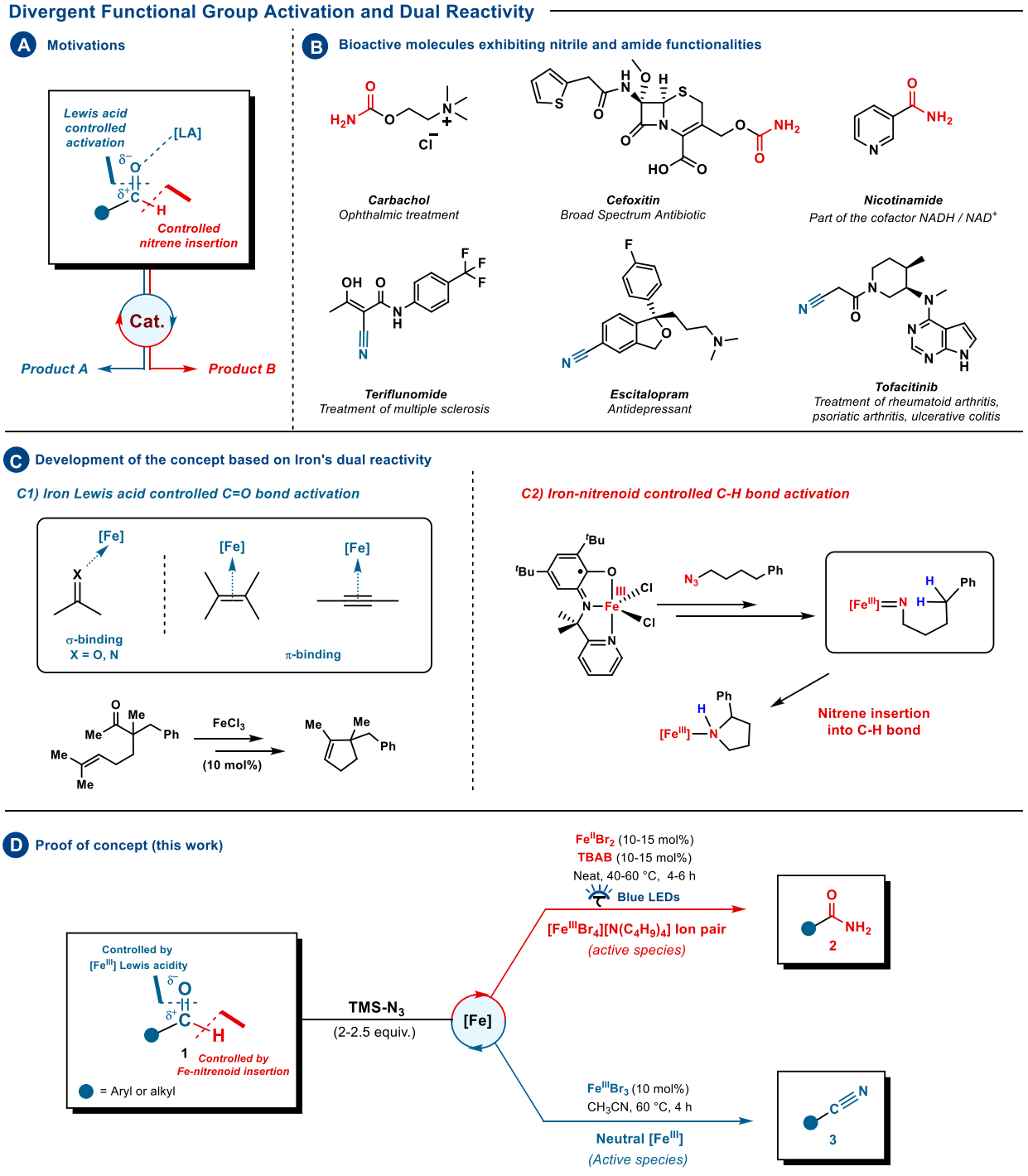

transformations. Self-adjustment constitutes an essential prerequisite in the perspective of developing effective universal catalysts. In the laboratories, efforts to conceive such systems would advance the fundamental understanding of the necessary requirements to control different chemical transformation sequences, ultimately producing selectively different products from a large panel of building blocks.

Here, we envisaged whether a catalyst might, depending on the reaction conditions, open divergent reaction pathways by engaging different intrinsic chemical bonds of a primary functional group (e.g., aldehyde; Scheme 1, panel A). Specifically, in the case of aldehydes, such a system would be able to separately address either the C═O (Scheme 1, panel A, blue) or C−H bond (Scheme 1, panel A, red) to offer various products.

To probe the feasibility of the concept, the controlled insertion of nitrogen moieties in the form of nitrile or amide groups into aldehyde starting materials constitutes an attractive scenario because nitrogen-containing motifs are found in many life science molecules, natural products, drugs, and materials (Scheme 1, panel B).[6] Conventional methods for their preparation include, among others,[7] Schmidt-type reactions that convert carbonyl functionalities (e.g., aldehydes, ketones) in the desired products by using hydrazoic acid or organic

https://doi.org/10.1021/acscatal.1c00733
ACS Catal. 2021, 11, 7176−7185

Scheme 2. Substrate Scope of Amides and Nitriles under Optimized Protocols

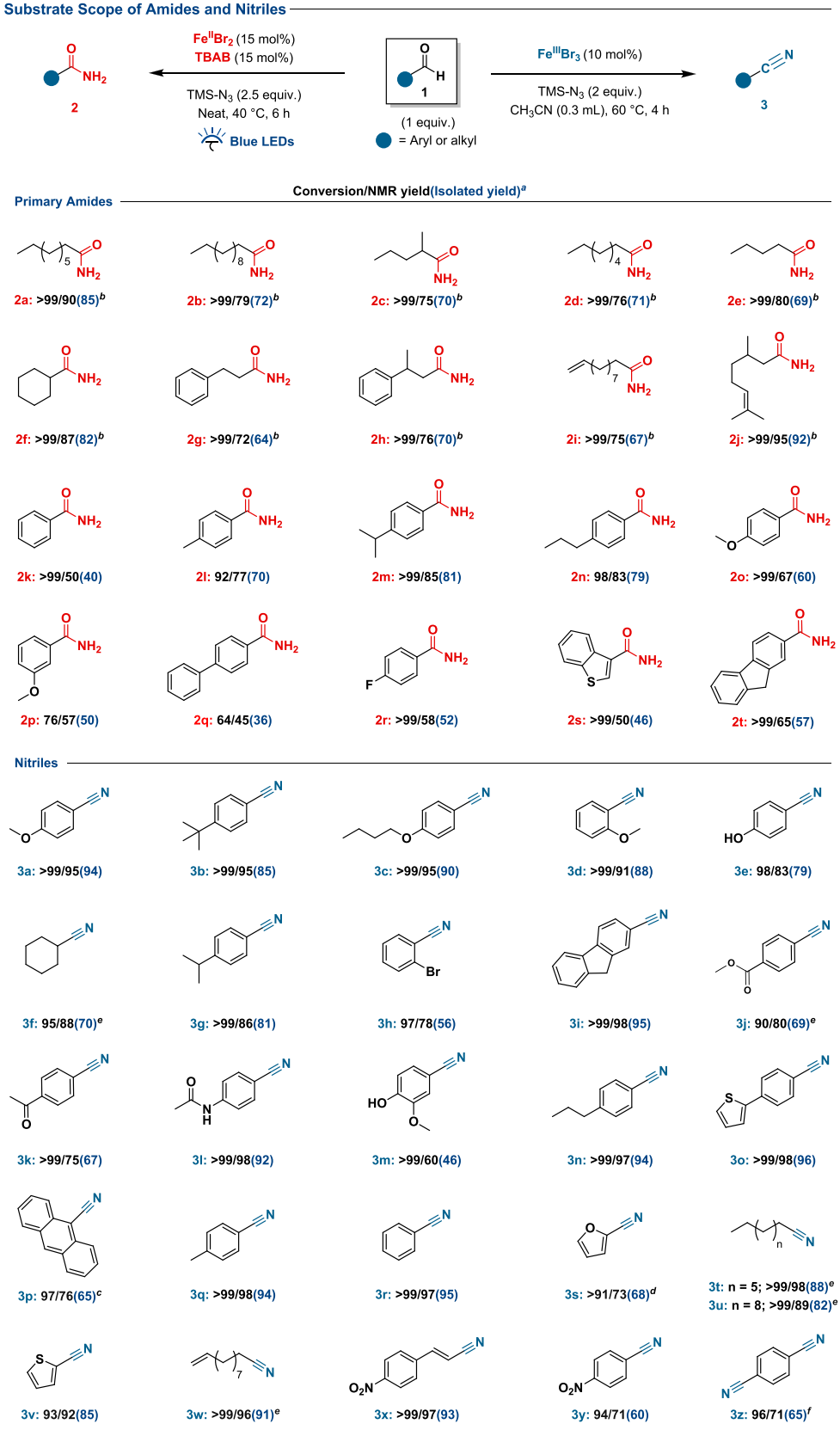

[a]Conversions (%) and yields (%) are based on ^{1}H NMR relative to mesitylene (0.5 mmol) as an internal standard; isolated yields (%) are given in brackets. [b]Modified conditions: $FeBr_2$ (10 mol%), TBAB (10 mol%), TMS-N_3 (2 equiv), 60 °C, 4 h. [c]The reaction was performed for 14 h. [d]The reaction was performed at 25 °C for 20 h. [e]Modified conditions: $FeBr_3$ (10 mol%), TMS-N_3 (2 equiv), 80 °C, 4 h. [f]Modified conditions: $FeBr_3$ (20 mol%), TMS-N_3 (4 equiv), 60 °C, 14 h; we note the formation of mononitrile (25%).

https://doi.org/10.1021/acscatal.1c00733
ACS Catal. 2021, 11, 7176−7185

Table 1. Optimization of the Reaction Conditions for Amide and Nitrile Synthesis

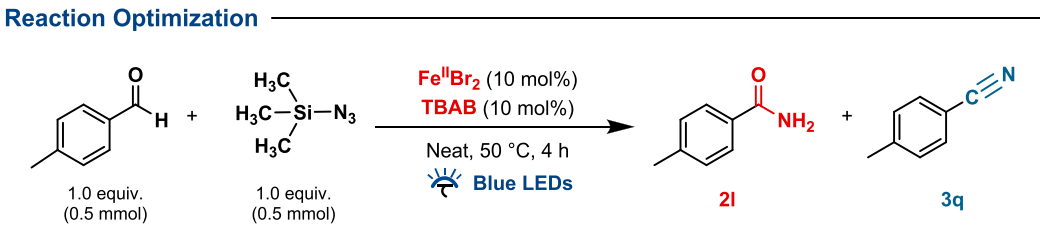

Entry	Deviation from Above	Yields (%)[a] 2l:3q
1	None	50:4
2	No $Fe^{II}Br_2$	0:0
3	No $Fe^{II}Br_2$ / No TBAB	0:0
4	No $Fe^{II}Br_2$ / No blue LEDs / CH_3CN (0.3 mL)	0:0
5	CH_3CN (0.3 mL)	51:5
6	Dioxane (0.3 mL)	40:4
7	No blue LEDs	39:4
8	UV (365 nm) light	38:6
9	Molecular Sieves (3 Å)	36:7
10	TMS-N_3 (1.5 equiv.)	60:4
11	TMS-N_3 (2.0 equiv.)	68:3
12	TMS-N_3 (2.0 equiv.) / 60 °C	70:6
13	$Fe^{II}Br_2$ (15 mol%) / TBAB (15 mol%) / TMS-N_3 (2.0 equiv.) / 60 °C / 2 h	67:7
14	**$Fe^{II}Br_2$ (15 mol%) / TBAB (15 mol%) / TMS-N_3 (2.5 equiv.) / 40 °C / 6 h**	**77:4**
15	$Fe^{III}Br_3$ (10 mol%) / No TBAB / CH_3CN (0.3 mL)	0:73
16	$Fe^{III}Br_3$ (10 mol%) / CH_3CN (0.3 mL)	3:15
17	$Fe^{III}Br_3$ (10 mol%) / No blue LEDs / CH_3CN (0.3 mL)	0:44
18	$Fe^{III}Br_3$ (10 mol%) / No TBAB / No blue LEDs / CH_3CN (0.3 mL)	0:71
19	$Fe^{III}Br_3$ (10 mol%) / No TBAB / No blue LEDs / CH_3CN (0.3 mL) / TMS-N_3 (2.0 equiv.)	0:94
20	**$Fe^{III}Br_3$ (10 mol%) / No TBAB / No blue LEDs / CH_3CN (0.3 mL) / TMS-N_3 (2.0 equiv.) / 60 °C**	**0:98**

[a]Yields are based on ^{1}H NMR relative to mesitylene (0.5 mmol) as an internal standard.

azides as nitrogen sources.[8] In these approaches, selectivity remains a critical challenge, and protocols providing both products remain elusive.[9]

Pursuing this idea, we set out to explore iron as a potential catalyst and trimethylsilylazide (TMS-N_3) as a masked source of primary nitrogen. The choice of this specific combination of metal/N source stems from their mutually compatible dual reactivities. Iron has established itself as (1) a Lewis acid[10] capable of activating carbonyl units (Scheme 1, panel C1)[11] and as (2) a versatile platform for the generation, transfer, and insertion of nitrenoid species[12] into C−H bonds (Scheme 1, panel C2).[13] Reciprocally, TMS-N_3 can act both as a nucleophile and as a nitrene source.[14]

On the basis of these considerations, we developed an operationally simple iron-based system that, depending on the reaction conditions, offers control over C═O versus C−H bond activation in aldehydes to convert a broad substrate scope to the desired amide and nitrile products in excellent yields under mild reaction conditions (Scheme 1, panel D).

RESULTS AND DISCUSSION

To assess the concept's feasibility, we first established the reaction conditions of the standard protocols applied in Scheme 2 derived from a detailed screening using 4-methylbenzaldehyde as a benchmark substrate; an abbreviated summary of the screening is represented in Table 1 (see the Supporting Information for more details). A myriad of metal precursors, reaction conditions, additives, and solvents were investigated, which revealed iron(II) bromide in the presence of tetra-*n*-butyl ammonium bromide (TBAB) as an optimal catalyst system for amide synthesis (Table 1, entry 14). In contrast, anhydrous iron(III) bromide performed best for the obtention of nitriles (Table 1, entry 20). In the case of amides, using light (λ_{max} = 455 nm) was found to be essential (Table 1, entries 1, 7, and 8), whereas temperature alone led to selectivity loss (Table 1, entry 7). Among all solvents screened, acetonitrile proved to be a valuable candidate (entry 5). However, the catalytic platform operates better under neat conditions, resulting in higher conversions and amide (**2l**) yields (see Table S4 for further information). Various tetra-*n*-butyl ammonium salts were evaluated as additives with the bromide derivative providing higher amide selectivity (Table S3). Finally, the reduction of the operating temperature to 40 °C delivered the standard reaction protocol for amide formation (Table 1, entry 14). Although TBAB emerged as an essential additive for amide formation, it seemingly does not benefit and even hampers nitrile formation (Table 1, entries 15 and 16). The nitrile product can be efficiently reached using

https://doi.org/10.1021/acscatal.1c00733
ACS Catal. 2021, 11, 7176−7185

Scheme 3. Empirical Mechanistic Investigations to Apprehend the Reaction Network

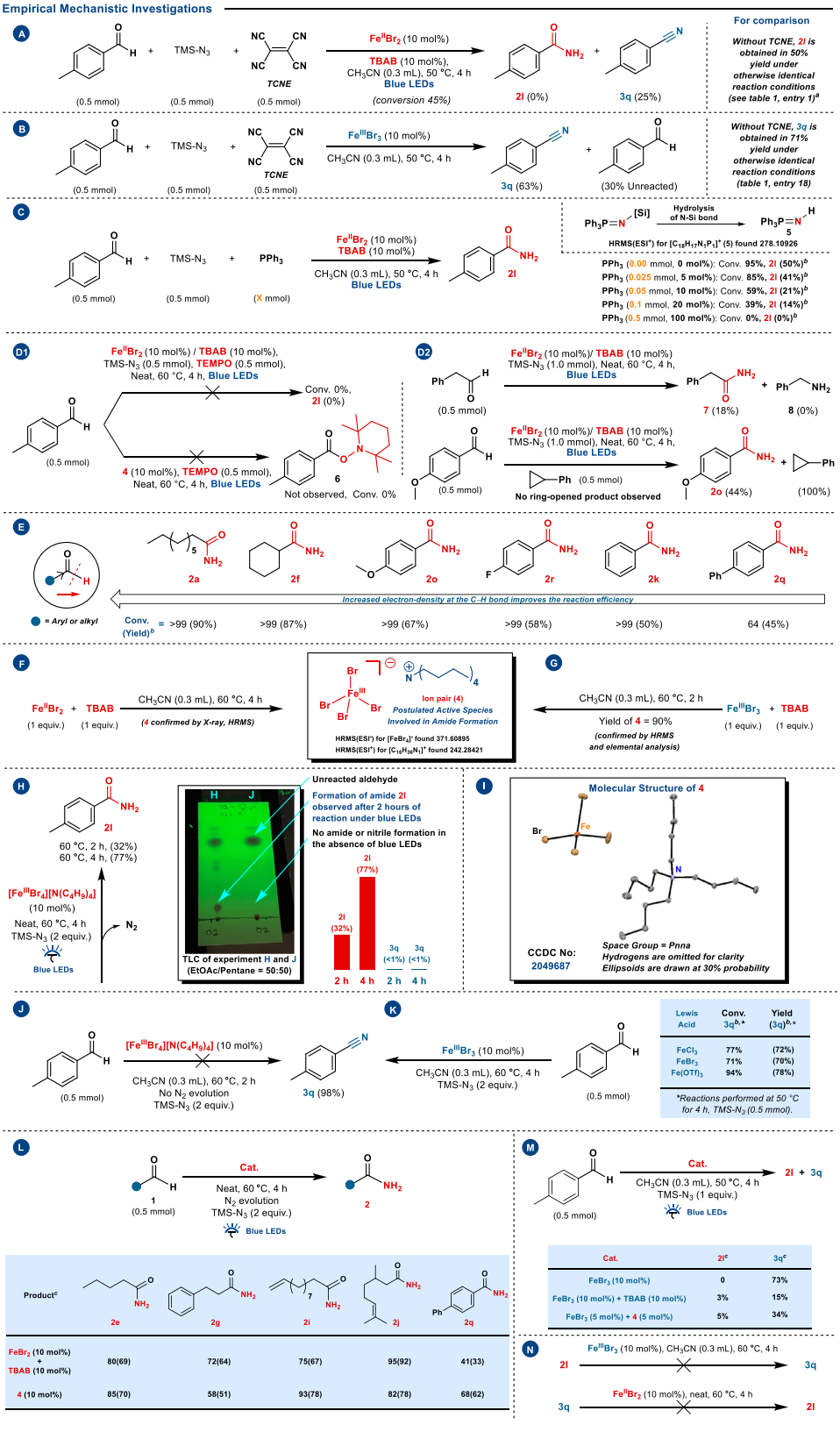

[a]Similarly, when using ion pair **4** instead of a $FeBr_2$/TBAB mixture, no amide formation could be observed (see the Supporting Information). [b]Conversions and/or yields (in brackets) are based on ^1H NMR relative to mesitylene (0.5 mmol) as an internal standard. [c]Yields are based on ^1H NMR relative to mesitylene (0.5 mmol) as an internal standard. Isolated yields are given in brackets.

https://doi.org/10.1021/acscatal.1c00733
ACS Catal. 2021, 11, 7176−7185

Scheme 4. Proposed Reaction Pathways for Amide and Nitrile Formation

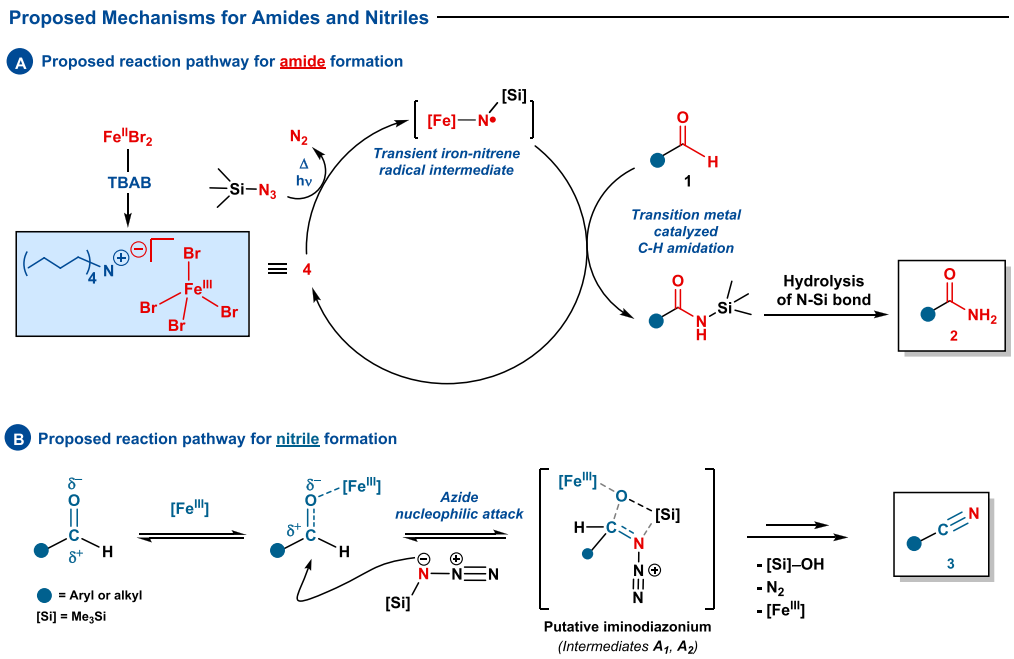

Lewis acidic FeX_3 salts (X = Cl, Br, OTf; see Table S2 for further information) without any additives or a light source (Table 1, entries 18−20). The final set of the reaction conditions for both products is functional under an argon atmosphere, leading to the completion of the reactions in 4−6 h, and can be set up in minutes using a commercially available photoreactor (see Figure S1 for details about the setup).

With the optimized reaction conditions in hand (Table 1, entries 14 and 20), we investigated the substrate scope to assess this protocol's generality (Scheme 2). Substrates embedded with different functionalities endured the reaction efficiently, demonstrating the viability of the procedure. For both amides and nitriles, aliphatic and aromatic derivatives could be employed. Aliphatic aldehydes supplied better results for amides when reducing the catalyst loading (10 mol %). In contrast, aromatic derivatives required slightly increased amounts of catalyst (15 mol %) and TMS-N_3 (2.5 equiv). Interestingly, olefinic substituents were well-tolerated and supplied the targeted amides selectively (**2i**−**j**). Also, heteroarenes (**2s**) and heteroatoms (**2o**−**p**, **2r**) containing substrates were amenable to amide formation. Similarly, in the case of the nitriles, heteroarenes (**3o**, **3s**, **3v**) and substrates featuring alkoxy (**3a**, **3c**−**d**, **3m**), carbonyl (**3j**−**k**), amide (**3l**), or hydroxy (**3e**, **3m**) functionalities underwent the reaction efficiently. Aldehydes embedded with two formyl substituents also produced the corresponding dinitrile product (**3z**) selectively. Notably, substrates holding electron-donating groups (e.g., aliphatic, methoxy) offered higher selectivities and yields for amides. Oppositely, in the case of nitrile synthesis, compounds presenting electron-withdrawing functionalities showed better performances.

From a mechanistic standpoint, the developed iron-based system accomplishes the formal addition of a nitrogen atom to aldehydes supplying two different product platforms. In the case of amides, the reaction may proceed by inserting a metal-nitrenoid species into the aldehyde C−H bond. Similar intermediate species generated from azides under irradiation have been disclosed previously[15] and found competent to undergo C−H insertion reactions.[16] In contrast, the formation of nitriles may proceed through (1) activation of the aldehyde by the Lewis acidic iron(III) bromide; (2) nucleophilic attack of TMS-N_3; (3) hydrolysis. Several control experiments were designed and evaluated to supply empirical support for the proposed mechanisms (Scheme 3, panel A to N). First, the hypothesis of a putative iron−nitrenoid was tested by subjecting the catalyst system to tetracyanoethylene (TCNE), a nitrene trapping agent.[17] Under the established protocol for amide synthesis, with 4-methylbenzaldehyde as a substrate, the addition of TCNE led to a prohibition of product formation (Scheme 3, panel A). In contrast, TCNE presented no significant impact when applied to the nitrile protocol with **3q** forming in 63% instead of 71% yield (Scheme 3, panel B). These observations support that both products are generated through different mechanistic pathways. Next, the electrophilic nature of the putative nitrenoid species was verified by adding PPh_3 to the reaction mixture, a potent nucleophile capable of quenching electrophilic nitrenes (Scheme 3, panel C).[18] This led to an inhibition of amide formation along with the formation of $Ph_3P{=}NH$ (**5**) as detected by high-resolution mass spectrometry.[19] When performing the reaction in the presence of 2,2,6,6-tetramethylpiperidinyloxyl (TEMPO), no amide product was observed, further indicating the possible involvement of an iron−nitrene radical intermediate (Scheme 3, panel D1, top).[20] Additionally, TEMPO (Scheme 3, panel D1, bottom) and radical clock experiments (Scheme 3, panel D2)[20a,b,21] have not given any evidence regarding the implication of an acyl radical in the mechanistic picture. Finally, the evaluation of the structure−yield relationships among the amide products revealed that substrates embedded with electron-donating functionalities more efficiently endured the reaction (Scheme 3, panel E). This observation corroborates with a favored insertion of a putative electrophilic nitrenoid intermediate into electron-rich aldehyde C−H bonds.[22]

To probe the role of TBAB in amide formation, efforts were allocated to access the molecular identity of active species

https://doi.org/10.1021/acscatal.1c00733
ACS Catal. 2021, 11, 7176−7185

forming under operative conditions. When equimolar concentrations of $Fe^{II}Br_2$ and TBAB were mixed in an acetonitrile solution at 60 °C, the formation of an ion pair **4** was observed (Scheme 3, panel F).[23] The molecular identity of **4** could be confirmed by X-ray structure analysis (Scheme 3, panel I) and high-resolution mass spectrometry measurements as tetra-*n*-butylammonium iron tetrabromide (i.e., $[Fe^{III}Br_4][N(C_4H_9)_4]$). Similar species have been reported in the literature[24] and may result from the facile oxidation of iron(II) bromide in solution to a thermodynamically stable tetrabromoferrate(III) anion. Its formation may be influenced by various parameters such as solvent polarity, temperature, the excess of halide anions, or other coordinating functionalities.[25] Ion pair **4** can also be prepared in 90% yield by mixing equimolar amounts of $Fe^{III}Br_3$ and TBAB (Scheme 3, panel G). The catalytic relevance of ion pair **4** in the established protocol for amide synthesis was first examined using 4-methylbenzaldehyde as a substrate in the absence of added TBAB (Scheme 3, panel H). As expected, the exposure of the reaction mixture to light (i.e., blue LEDs) led to the formation of the corresponding amide **2l** in 32% yield after 2 h and further extending the reaction time to 4 h produced 77% of the product. Likewise, other substrates could also be converted by **4** to the expected products in yields similar to those obtained when using a mixture of $FeBr_2$ and TBAB (Scheme 3, panel L). In contrast, employing ion pair **4** as a catalyst for nitrile synthesis failed to produce **3q** (Scheme 3, panel J), thus confirming disparities in terms of reactivity and product selectivity between $[Fe^{III}Br_4][N(C_4H_9)_4]$ **4** and parent neutral $Fe^{III}X_3$ salts, which were all found to produce the desired nitrile under similar reaction conditions (Scheme 3, panel K). Complementarily, using equimolar quantities of **4** and $FeBr_3$ in the protocol for nitrile synthesis also hampered product formation (Scheme 3, panel M). This may be attributed to a decreased Lewis acidity of the tetravalent iron center. Finally, an implication of $Fe^{III}Br_3$ and $Fe^{II}Br_2$ salts in the interconversion of amides to nitriles and vice versa could be excluded (Scheme 3, panel N).

Therefore, it is postulated in Scheme 4 that the formation of amides and nitriles proceeds through two different reaction networks consistent with the preliminary control experiments (Scheme 3) and the temporal conversion profiles of the reactions (see the Supporting Information for more details). For amide formation (Scheme 4, panel A), $FeBr_2$ is proposed to first react with TBAB to produce the ion pair catalyst **4**. This species then activates TMS-N_3 with the contribution of an external stimulus such as light (λ_{max} = 455 nm) to provide a reactive iron−nitrene radical intermediate.[20a,b,26] Subsequently, its insertion into the aldehyde C−H bond generates an *N*-silylamide derivative, which offers the corresponding primary amide after hydrolysis. In contrast, when subjected to the standard set of reaction conditions for nitrile formation, $FeBr_3$ may react with the Lewis basic aldehyde *O*-donor center, which increases the electrophilicity of the adjacent carbon center (Scheme 4, panel B). This induces the nucleophilic attack of TMS-N_3 at the electron-deficient carbon atom, resulting in an intermediate species **A**, conceivably of iminodiazonium character,[27] which provides the corresponding nitrile after the liberation of N_2 and Me_3Si-OH.

CONCLUSION

In summary, we have developed an iron-based catalyst system, allowing for unique molecular control over product formation depending on the nature of the active species (i.e., neutral vs ion pair), which can be purposely generated and made operative under finely adjusted reaction conditions. The reported system demonstrates that primary functional groups can be controlled by specifically targeting their intrinsic chemical bonds to open divergent reaction pathways. More specifically, in the case of aldehydes, we have shown that addressing either the C═O or C−H bond can provide nitriles and amides in high yields and selectivities under mild reaction conditions. On the basis of preliminary mechanistic investigations, we propose that nitrile formation involves a neutral $Fe^{III}Br_3$ species acting as a Lewis acid that activates the aldehyde. This promotes the nucleophilic attack of TMS-N_3 and leads to the desired product after hydrolysis. In contrast, amide synthesis involves an in situ generated ion pair $[Fe^{III}Br_4][N(C_4H_9)_4]$. This species may then operate as a molecular platform capable of generating and transferring an electrophilic nitrene radical to the aldehyde C−H bond en route to the desired product. Further studies aiming to obtain more in-depth mechanistic information and extend this protocol to other functional groups are currently underway.

ASSOCIATED CONTENT

Supporting Information

The Supporting Information is available free of charge at https://pubs.acs.org/doi/10.1021/acscatal.1c00733.

General considerations, experimental methods and synthetic details, copies of NMR spectra, and crystallographic data for **4** (CCDC 2049687) (PDF)

AUTHOR INFORMATION

Corresponding Author

Christophe Werlé − *Max Planck Institute for Chemical Energy Conversion, 45470 Mülheim an der Ruhr, Germany; Ruhr University Bochum, 44801 Bochum, Germany;* orcid.org/0000-0002-2174-2148; Email: christophe.werle@cec.mpg.de

Authors

Basujit Chatterjee − *Max Planck Institute for Chemical Energy Conversion, 45470 Mülheim an der Ruhr, Germany; Ruhr University Bochum, 44801 Bochum, Germany;* orcid.org/0000-0003-3539-089X

Soumyashree Jena − *Max Planck Institute for Chemical Energy Conversion, 45470 Mülheim an der Ruhr, Germany; Ruhr University Bochum, 44801 Bochum, Germany*

Vishal Chugh − *Max Planck Institute for Chemical Energy Conversion, 45470 Mülheim an der Ruhr, Germany; Ruhr University Bochum, 44801 Bochum, Germany;* orcid.org/0000-0002-3875-4962

Thomas Weyhermüller − *Max Planck Institute for Chemical Energy Conversion, 45470 Mülheim an der Ruhr, Germany;* orcid.org/0000-0002-0399-7999

Complete contact information is available at: https://pubs.acs.org/10.1021/acscatal.1c00733

Author Contributions

#B.C. and S.J. contributed equally to this work.

Notes

The authors declare no competing financial interest.

https://doi.org/10.1021/acscatal.1c00733
ACS Catal. 2021, 11, 7176−7185

■ ACKNOWLEDGMENTS

We gratefully acknowledge the Max Planck Society for financial support and open access funding. We thank Prof. Dr. Walter Leitner for insightful discussions and generous support.

■ REFERENCES

(1) (a) McEvoy, J. P.; Brudvig, G. W. Water-splitting chemistry of photosystem II. *Chem. Rev.* **2006**, *106* (11), 4455−4483. (b) Thorseth, M. A.; Tornow, C. E.; Tse, E. C. M.; Gewirth, A. A. Cu complexes that catalyze the oxygen reduction reaction. *Coord. Chem. Rev.* **2013**, *257* (1), 130−139. (c) Broderick, J. B.; Duffus, B. R.; Duschene, K. S.; Shepard, E. M. Radical S-adenosylmethionine enzymes. *Chem. Rev.* **2014**, *114* (8), 4229−4317. (d) Lubitz, W.; Ogata, H.; Rudiger, O.; Reijerse, E. Hydrogenases. *Chem. Rev.* **2014**, *114* (8), 4081−4148. (e) Liu, J.; Chakraborty, S.; Hosseinzadeh, P.; Yu, Y.; Tian, S.; Petrik, I.; Bhagi, A.; Lu, Y. Metalloproteins containing cytochrome, iron-sulfur, or copper redox centers. *Chem. Rev.* **2014**, *114* (8), 4366−4469. (f) Solomon, E. I.; Heppner, D. E.; Johnston, E. M.; Ginsbach, J. W.; Cirera, J.; Qayyum, M.; Kieber-Emmons, M. T.; Kjaergaard, C. H.; Hadt, R. G.; Tian, L. Copper active sites in biology. *Chem. Rev.* **2014**, *114* (7), 3659−3853. (g) Wang, V. C.; Maji, S.; Chen, P. P.; Lee, H. K.; Yu, S. S.; Chan, S. I. Alkane Oxidation: Methane Monooxygenases, Related Enzymes, and Their Biomimetics. *Chem. Rev.* **2017**, *117* (13), 8574−8621. (h) Seefeldt, L. C.; Hoffman, B. M.; Peters, J. W.; Raugei, S.; Beratan, D. N.; Antony, E.; Dean, D. R. Energy Transduction in Nitrogenase. *Acc. Chem. Res.* **2018**, *51* (9), 2179−2186. (i) Dunham, N. P.; Arnold, F. H. Nature's Machinery, Repurposed: Expanding the Repertoire of Iron-Dependent Oxygenases. *ACS Catal.* **2020**, *10* (20), 12239−12255. (j) Van Stappen, C.; Decamps, L.; Cutsail, G. E., 3rd; Bjornsson, R.; Henthorn, J. T.; Birrell, J. A.; DeBeer, S. The Spectroscopy of Nitrogenases. *Chem. Rev.* **2020**, *120* (12), 5005−5081.

(2) Cornils, B.; Herrmann, W. A.; Beller, M.; Paciello, R. *Applied homogeneous catalysis with organometallic compounds: a comprehensive handbook in four volumes*; Wiley-VCH Verlag GmbH & Co. KGaA: Weinheim, 2018.

(3) (a) Wang, X.; Thevenon, A.; Brosmer, J. L.; Yu, I.; Khan, S. I.; Mehrkhodavandi, P.; Diaconescu, P. L. Redox control of group 4 metal ring-opening polymerization activity toward L-lactide and epsilon-caprolactone. *J. Am. Chem. Soc.* **2014**, *136* (32), 11264−11267. (b) Rodrigues, R. R.; Boudreaux, C. M.; Papish, E. T.; Delcamp, J. H. Photocatalytic Reduction of CO_2 to CO and Formate: Do Reaction Conditions or Ruthenium Catalysts Control Product Selectivity? *ACS Appl. Energy Mater.* **2019**, *2* (1), 37−46. (c) Goswami, A.; Paululat, T.; Schmittel, M. Switching Dual Catalysis without Molecular Switch: Using A Multicomponent Information System for Reversible Reconfiguration of Catalytic Machinery. *J. Am. Chem. Soc.* **2019**, *141* (39), 15656−15663. (d) Bhattacharya, M.; Sebghati, S.; VanderLinden, R. T.; Saouma, C. T. Toward Combined Carbon Capture and Recycling: Addition of an Amine Alters Product Selectivity from CO to Formic Acid in Manganese Catalyzed Reduction of CO_2. *J. Am. Chem. Soc.* **2020**, *142* (41), 17589−17597. (e) Cramer, H. H.; Chatterjee, B.; Weyhermuller, T.; Werlé, C.; Leitner, W. Controlling the Product Platform of Carbon Dioxide Reduction: Adaptive Catalytic Hydrosilylation of CO_2 Using a Molecular Cobalt(II) Triazine Complex. *Angew. Chem., Int. Ed.* **2020**, *59* (36), 15674−15681. (f) Sulley, G. S.; Gregory, G. L.; Chen, T. T. D.; Pena Carrodeguas, L.; Trott, G.; Santmarti, A.; Lee, K. Y.; Terrill, N. J.; Williams, C. K. Switchable Catalysis Improves the Properties of CO_2-Derived Polymers: Poly(cyclohexene carbonate-b-epsilon-decalactone-b-cyclohexene carbonate) Adhesives, Elastomers, and Toughened Plastics. *J. Am. Chem. Soc.* **2020**, *142* (9), 4367−4378.

(4) (a) Lehn, J. M. Perspectives in chemistry−aspects of adaptive chemistry and materials. *Angew. Chem., Int. Ed.* **2015**, *54* (11), 3276−3289. (b) Chatterjee, B.; Chang, W. C.; Werlé, C. Molecularly Controlled Catalysis - Targeting Synergies Between Local and Non-local Environments. *ChemCatChem* **2021**, *13*, 1659. (c) Chatterjee, B.; Chang, W. C.; Jena, S.; Werlé, C. Implementation of Cooperative Designs in Polarized Transition Metal Systems-Significance for Bond Activation and Catalysis. *ACS Catal.* **2020**, *10* (23), 14024−14055.

(5) (a) Blanco, V.; Leigh, D. A.; Marcos, V. Artificial switchable catalysts. *Chem. Soc. Rev.* **2015**, *44* (15), 5341−5370. (b) Teator, A. J.; Lastovickova, D. N.; Bielawski, C. W. Switchable Polymerization Catalysts. *Chem. Rev.* **2016**, *116* (4), 1969−1992. (c) Mendelsohn, L. N.; MacNeil, C. S.; Tian, L.; Park, Y.; Scholes, G. D.; Chirik, P. J. Visible-Light-Enhanced Cobalt-Catalyzed Hydrogenation: Switchable Catalysis Enabled by Divergence between Thermal and Photochemical Pathways. *ACS Catal.* **2021**, *11* (3), 1351−1360.

(6) (a) Smolen, V. F.; Clevenger, J. M.; Williams, E. J.; Bergdolt, M. W. Biophasic availability of ophthalmic carbachol. I. Mechanisms of cationic polymer- and surfactant-promoted miotic activity. *J. Pharm. Sci.* **1973**, *62* (6), 958−961. (b) Gootz, T. D. Discovery and development of new antimicrobial agents. *Clin. Microbiol. Rev.* **1990**, *3* (1), 13−31. (c) Breedveld, F. C.; Dayer, J. M. Leflunomide: mode of action in the treatment of rheumatoid arthritis. *Ann. Rheum. Dis.* **2000**, *59* (11), 841−849. (d) Miller, J. S.; Manson, J. L. Designer magnets containing cyanides and nitriles. *Acc. Chem. Res.* **2001**, *34* (7), 563−570. (e) Hili, R.; Yudin, A. K. Making carbon-nitrogen bonds in biological and chemical synthesis. *Nat. Chem. Biol.* **2006**, *2* (6), 284−287. (f) Belenky, P.; Bogan, K. L.; Brenner, C. NAD^+ metabolism in health and disease. *Trends Biochem. Sci.* **2007**, *32* (1), 12−19. (g) Fleming, F. F.; Yao, L.; Ravikumar, P. C.; Funk, L.; Shook, B. C. Nitrile-containing pharmaceuticals: efficacious roles of the nitrile pharmacophore. *J. Med. Chem.* **2010**, *53* (22), 7902−7917. (h) McGrath, N. A.; Brichacek, M.; Njardarson, J. T. A Graphical Journey of Innovative Organic Architectures That Have Improved Our Lives. *J. Chem. Educ.* **2010**, *87* (12), 1348−1349. (i) Adis, E. Tofacitinib. *Drugs R&D* **2010**, *10* (4), 271−284. (j) Pattabiraman, V. R.; Bode, J. W. Rethinking amide bond synthesis. *Nature* **2011**, *480* (7378), 471−479. (k) Bostrom, J.; Brown, D. G.; Young, R. J.; Keseru, G. M. Expanding the medicinal chemistry synthetic toolbox. *Nat. Rev. Drug Discovery* **2018**, *17* (10), 709−727. (l) Cipriani, A.; Furukawa, T. A.; Salanti, G.; Chaimani, A.; Atkinson, L. Z.; Ogawa, Y.; Levcht, S.; Ruhe, H. G.; Turner, E. H.; Higgins, J. P. T.; Egger, M.; Takeshima, N.; Hayasaka, Y.; Imai, H.; Shinohara, K.; Tajika, A.; Ioannidis, J. P. A.; Geddes, J. R. Comparative efficacy and acceptability of 21 antidepressant drugs for the acute treatment of adults with major depressive disorder: a systematic review and network meta-analysis. *Lancet* **2018**, *391* (10128), 1357−1366. (m) *Njardarson Website: Top200 Small Molecule Pharmaceuticals by Retail Sales in 2018*; https://njardarson.lab.arizona.edu/.

(7) (a) Blatt, A. H. The Beckmann rearrangement. *Chem. Rev.* **1933**, *12* (2), 215−260. (b) Mowry, D. T. The preparation of nitriles. *Chem. Rev.* **1948**, *42* (2), 189−283. (c) Ellis, G. P.; Romney-Alexander, T. M. Cyanation of aromatic halides. *Chem. Rev.* **1987**, *87* (4), 779−794. (d) Zhou, W.; Zhang, L.; Jiao, N. Direct transformation of methyl arenes to aryl nitriles at room temperature. *Angew. Chem., Int. Ed.* **2009**, *48* (38), 7094−7097. (e) Valeur, E.; Bradley, M. Amide bond formation: beyond the myth of coupling reagents. *Chem. Soc. Rev.* **2009**, *38* (2), 606−631. (f) Anbarasan, P.; Schareina, T.; Beller, M. Recent developments and perspectives in palladium-catalyzed cyanation of aryl halides: synthesis of benzonitriles. *Chem. Soc. Rev.* **2011**, *40* (10), 5049−5067. (g) Allen, C. L.; Williams, J. M. Metal-catalysed approaches to amide bond formation. *Chem. Soc. Rev.* **2011**, *40* (7), 3405−3415. (h) Kim, J.; Kim, H. J.; Chang, S. Synthesis of aromatic nitriles using nonmetallic cyano-group sources. *Angew. Chem., Int. Ed.* **2012**, *51* (48), 11948−11959. (i) Lundberg, H.; Tinnis, F.; Selander, N.; Adolfsson, H. Catalytic amide formation from non-activated carboxylic acids and amines. *Chem. Soc. Rev.* **2014**, *43* (8), 2714−2742. (j) de Figueiredo, R. M.; Suppo, J. S.; Campagne, J. M. Nonclassical Routes for Amide Bond Formation. *Chem. Rev.* **2016**, *116* (19), 12029−12122. (k) Ping, Y. Y.; Ding, Q. P.; Peng, Y. Y. Advances in C-CN Bond Formation via C-H Bond Activation. *ACS Catal.* **2016**, *6* (9), 5989−6005. (l) Yan, G. B.; Zhang, Y.; Wang, J. B. Recent Advances in the Synthesis of Aryl Nitrile Compounds. *Adv. Synth. Catal.* **2017**, *359* (23), 4068−4105. (m) Narendar Reddy, T.;

https://doi.org/10.1021/acscatal.1c00733
ACS Catal. 2021, 11, 7176−7185

Beatriz, A.; Jayathirtha Rao, V.; de Lima, D. P. Carbonyl Compounds' Journey to Amide Bond Formation. *Chem. - Asian J.* **2019**, *14* (3), 344−388.
(8) (a) Schmidt, K. F. Über den Imin-Rest. *Ber. Dtsch. Chem. Ges. B* **1924**, *57* (4), 704−706. (b) Smith, P. A. S. The Schmidt Reaction - Experimental Conditions and Mechanism. *J. Am. Chem. Soc.* **1948**, *70* (1), 320−323. (c) McEwen, W. E.; Conrad, W. E.; VanderWerf, C. A. The Schmidt Reaction Applied to Aldehydes and Epoxides1. *J. Am. Chem. Soc.* **1952**, *74* (5), 1168−1171. (d) Nishiyama, K.; Oba, M.; Watanabe, A. Reactions of Trimethylsilyl Azide with Aldehydes - Facile and Convenient Syntheses of Diazides, Tetrazoles, and Nitriles. *Tetrahedron* **1987**, *43* (4), 693−700. (e) Hoffman, R. V.; Salvador, J. M. Cationic Carbon to Nitrogen Rearrangements in the Reactions of N-(Sulfonyloxy)Amines with Aldehydes. *J. Org. Chem.* **1992**, *57* (16), 4487−4490. (f) Aube, J.; Milligan, G. L. Intramolecular Schmidt reaction of alkyl azides. *J. Am. Chem. Soc.* **1991**, *113* (23), 8965−8966. (g) Pearson, W. H.; Walavalkar, R.; Schkeryantz, J. M.; Fang, W. K.; Blickensdorf, J. D. Intramolecular Schmidt reactions of azides with carbocations: synthesis of bridged-bicyclic and fused-bicyclic tertiary amines. *J. Am. Chem. Soc.* **1993**, *115* (22), 10183−10194. (h) Milligan, G. L.; Mossman, C. J.; Aube, J. Intramolecular Schmidt Reactions of Alkyl Azides with Ketones: Scope and Stereochemical Studies. *J. Am. Chem. Soc.* **1995**, *117* (42), 10449−10459. (i) Gorin, D. J.; Davis, N. R.; Toste, F. D. Gold(I)-catalyzed intramolecular acetylenic Schmidt reaction. *J. Am. Chem. Soc.* **2005**, *127* (32), 11260−11261. (j) Wolff, H. The Schmidt Reaction. In *Organic Reactions*; Wiley, 2011; pp 307−336;. (k) Liu, R.; Gutierrez, O.; Tantillo, D. J.; Aube, J. Stereocontrol in a combined allylic azide rearrangement and intramolecular Schmidt reaction. *J. Am. Chem. Soc.* **2012**, *134* (15), 6528−6531.
(9) (a) Khalafi-Nezhad, A.; Mohammadi, S. Chitosan supported ionic liquid: a recyclable wet and dry catalyst for the direct conversion of aldehydes into nitriles and amides under mild conditions. *RSC Adv.* **2014**, *4* (27), 13782−13787. (b) Murugesan, K.; Senthamarai, T.; Sohail, M.; Sharif, M.; Kalevaru, N. V.; Jagadeesh, R. V. Stable and reusable nanoscale Fe_2O_3-catalyzed aerobic oxidation process for the selective synthesis of nitriles and primary amides. *Green Chem.* **2018**, *20* (1), 266−273. (c) Liu, J.; Zhang, C.; Zhang, Z.; Wen, X.; Dou, X.; Wei, J.; Qiu, X.; Song, S.; Jiao, N. Nitromethane as a nitrogen donor in Schmidt-type formation of amides and nitriles. *Science* **2020**, *367* (6475), 281−285.
(10) (a) Bolm, C.; Legros, J.; Le Paih, J.; Zani, L. Iron-catalyzed reactions in organic synthesis. *Chem. Rev.* **2004**, *104* (12), 6217−6254. (b) Vrancken, E.; Campagne, J.-M. Organic Transformations Promoted by Lewis Acid Iron Catalysts. In *PATAI'S Chemistry of Functional Groups*; Wiley, 2013; DOI: 10.1002/9780470682531.pat0656. (c) Bauer, I.; Knolker, H. J. Iron catalysis in organic synthesis. *Chem. Rev.* **2015**, *115* (9), 3170−3387. (d) Fürstner, A. Iron Catalysis in Organic Synthesis: A Critical Assessment of What It Takes To Make This Base Metal a Multitasking Champion. *ACS Cent. Sci.* **2016**, *2* (11), 778−789. (e) Ollevier, T. *Iron-based Chiral Lewis Acids*; Wiley, 2017; pp 59−101; DOI: 10.1002/9783527802142.ch3.
(11) Albright, H.; Riehl, P. S.; McAtee, C. C.; Reid, J. P.; Ludwig, J. R.; Karp, L. A.; Zimmerman, P. M.; Sigman, M. S.; Schindler, C. S. Catalytic Carbonyl-Olefin Metathesis of Aliphatic Ketones: Iron(III) Homo-Dimers as Lewis Acidic Superelectrophiles. *J. Am. Chem. Soc.* **2019**, *141* (4), 1690−1700.
(12) (a) Kuijpers, P. F.; van der Vlugt, J. I.; Schneider, S.; de Bruin, B. Nitrene Radical Intermediates in Catalytic Synthesis. *Chem. - Eur. J.* **2017**, *23* (56), 13819−13829. (b) Wilding, M. J. T.; Iovan, D. A.; Betley, T. A. High-Spin Iron Imido Complexes Competent for C-H Bond Amination. *J. Am. Chem. Soc.* **2017**, *139* (34), 12043−12049. (c) Plietker, B.; Roske, A. Recent advances in Fe-catalyzed C-H aminations using azides as nitrene precursors. *Catal. Sci. Technol.* **2019**, *9* (16), 4188−4197. (d) Du, Y. D.; Zhou, C. Y.; To, W. P.; Wang, H. X.; Che, C. M. Iron porphyrin catalysed light driven C-H bond amination and alkene aziridination with organic azides. *Chem. Sci.* **2020**, *11* (18), 4680−4686. (e) Das, S. K.; Roy, S.; Khatua, H.; Chattopadhyay, B. Iron-Catalyzed Amination of Strong Aliphatic C(sp^3)-H Bonds. *J. Am. Chem. Soc.* **2020**, *142* (38), 16211−16217.
(13) Bagh, B.; Broere, D. L. J.; Sinha, V.; Kuijpers, P. F.; van Leest, N. P.; de Bruin, B.; Demeshko, S.; Siegler, M. A.; van der Vlugt, J. I. Catalytic Synthesis of N-Heterocycles via Direct C(sp^3)-H Amination Using an Air-Stable Iron(III) Species with a Redox-Active Ligand. *J. Am. Chem. Soc.* **2017**, *139* (14), 5117−5124.
(14) (a) Groutas, W. C.; Felker, D. Synthetic Applications of Cyanotrimethylsilane, Iodotrimethylsilane, Azidotrimethylsilane, and Methylthiotrimethylsilane. *Synthesis* **1980**, *1980* (11), 861−868. (b) Scriven, E. F. V.; Turnbull, K. Azides - Their Preparation and Synthetic Uses. *Chem. Rev.* **1988**, *88* (2), 297−368. (c) Brase, S.; Gil, C.; Knepper, K.; Zimmermann, V. Organic azides: an exploding diversity of a unique class of compounds. *Angew. Chem., Int. Ed.* **2005**, *44* (33), 5188−5240. (d) Cenini, S.; Gallo, E.; Caselli, A.; Ragaini, F.; Fantauzzi, S.; Piangiolino, C. Coordination chemistry of organic azides and amination reactions catalyzed by transition metal complexes. *Coord. Chem. Rev.* **2006**, *250* (11−12), 1234−1253. (e) Lang, S.; Murphy, J. A. Azide rearrangements in electron-deficient systems. *Chem. Soc. Rev.* **2006**, *35* (2), 146−156. (f) Intrieri, D.; Zardi, P.; Caselli, A.; Gallo, E. Organic azides: ″energetic reagents″ for the intermolecular amination of C-H bonds. *Chem. Commun. (Cambridge, U. K.)* **2014**, *50* (78), 11440−11453. (g) Davies, P. W.; Garzón, M. Nucleophilic Nitrenoids Through π-Acid Catalysis: Providing a Common Basis for Rapid Access into Diverse Nitrogen Heterocycles. *Asian J. Org. Chem.* **2015**, *4* (8), 694−708.
(15) (a) Wagner, W. D.; Nakamoto, K. Formation of nitridoiron(V) porphyrins detected by resonance Raman spectroscopy. *J. Am. Chem. Soc.* **1988**, *110* (12), 4044−4045. (b) Wagner, W. D.; Nakamoto, K. Resonance Raman spectra of nitridoiron(V) porphyrin intermediates produced by laser photolysis. *J. Am. Chem. Soc.* **1989**, *111* (5), 1590−1598. (c) Betley, T. A.; Peters, J. C. A tetrahedrally coordinated L_3Fe-N_x platform that accommodates terminal nitride ($Fe^{IV}N$) and dinitrogen (Fe^{I}-N_2-Fe^{I}) ligands. *J. Am. Chem. Soc.* **2004**, *126* (20), 6252−6254. (d) Aliaga-Alcalde, N.; George, S. D.; Mienert, B.; Bill, E.; Wieghardt, K.; Neese, F. The geometric and electronic structure of [(cyclam-acetato)Fe(N)]$^+$: a genuine iron(v) species with a ground-state spin $S = 1/2$. *Angew. Chem., Int. Ed.* **2005**, *44* (19), 2908−2912. (e) Berry, J. F.; Bill, E.; Bothe, E.; George, S. D.; Mienert, B.; Neese, F.; Wieghardt, K. An octahedral coordination complex of iron(VI). *Science* **2006**, *312* (5782), 1937−1941. (f) Cowley, R. E.; Bill, E.; Neese, F.; Brennessel, W. W.; Holland, P. L. Iron(II) complexes with redox-active tetrazene (RNNNNR) ligands. *Inorg. Chem.* **2009**, *48* (11), 4828−4836. (g) Hohenberger, J.; Ray, K.; Meyer, K. The biology and chemistry of high-valent iron-oxo and iron-nitrido complexes. *Nat. Commun.* **2012**, *3* (1), 720. (h) Hong, S.; Sutherlin, K. D.; Vardhaman, A. K.; Yan, J. J.; Park, S.; Lee, Y. M.; Jang, S.; Lu, X.; Ohta, T.; Ogura, T.; Solomon, E. I.; Nam, W. A Mononuclear Nonheme Iron(V)-Imido Complex. *J. Am. Chem. Soc.* **2017**, *139* (26), 8800−8803. (i) Sabenya, G.; Lazaro, L.; Gamba, I.; Martin-Diaconescu, V.; Andris, E.; Weyhermuller, T.; Neese, F.; Roithova, J.; Bill, E.; Lloret-Fillol, J.; Costas, M. Generation, Spectroscopic, and Chemical Characterization of an Octahedral Iron(V)-Nitrido Species with a Neutral Ligand Platform. *J. Am. Chem. Soc.* **2017**, *139* (27), 9168−9177. (j) Lu, X.; Li, X. X.; Lee, Y. M.; Jang, Y.; Seo, M. S.; Hong, S.; Cho, K. B.; Fukuzumi, S.; Nam, W. Electron-Transfer and Redox Reactivity of High-Valent Iron Imido and Oxo Complexes with the Formal Oxidation States of Five and Six. *J. Am. Chem. Soc.* **2020**, *142* (8), 3891−3904. (k) Martinez, J. L.; Lutz, S. A.; Yang, H.; Xie, J.; Telser, J.; Hoffman, B. M.; Carta, V.; Pink, M.; Losovyj, Y.; Smith, J. M. Structural and spectroscopic characterization of an Fe(VI) bis(imido) complex. *Science* **2020**, *370* (6514), 356−359. (l) Keilwerth, M.; Grunwald, L.; Mao, W.; Heinemann, F. W.; Sutter, J.; Bill, E.; Meyer, K. Ligand Tailoring Toward an Air-Stable Iron(V) Nitrido Complex. *J. Am. Chem. Soc.* **2021**, *143* (3), 1458−1465.
(16) (a) Stella, L. Homolytic Cyclizations of N-Chloroalkenylamines. *Angew. Chem., Int. Ed. Engl.* **1983**, *22* (5), 337−350. (b) Eikey, R. A.; Abu-Omar, M. M. Nitrido and imido transition

https://doi.org/10.1021/acscatal.1c00733
ACS Catal. 2021, 11, 7176−7185

metal complexes of Groups 6−8. *Coord. Chem. Rev.* **2003**, *243* (1−2), 83−124. (c) Moreau, Y.; Chen, H.; Derat, E.; Hirao, H.; Bolm, C.; Shaik, S. NR transfer reactivity of azo-compound I of P450. How does the nitrogen substituent tune the reactivity of the species toward C-H and C = C activation? *J. Phys. Chem. B* **2007**, *111* (34), 10288−10299. (d) Zard, S. Z. Recent progress in the generation and use of nitrogen-centred radicals. *Chem. Soc. Rev.* **2008**, *37* (8), 1603−1618. (e) Davies, H. M.; Manning, J. R. Catalytic C-H functionalization by metal carbenoid and nitrenoid insertion. *Nature* **2008**, *451* (7177), 417−424. (f) King, E. R.; Hennessy, E. T.; Betley, T. A. Catalytic C−H Bond Amination from High-Spin Iron Imido Complexes. *J. Am. Chem. Soc.* **2011**, *133* (13), 4917−4923. (g) Paradine, S. M.; White, M. C. Iron-catalyzed intramolecular allylic C-H amination. *J. Am. Chem. Soc.* **2012**, *134* (4), 2036−2039. (h) Liu, Y.; Guan, X.; Wong, E. L.; Liu, P.; Huang, J. S.; Che, C. M. Nonheme iron-mediated amination of C(sp^3)-H bonds. Quinquepyridine-supported iron-imide/nitrene intermediates by experimental studies and DFT calculations. *J. Am. Chem. Soc.* **2013**, *135* (19), 7194−7204. (i) Nguyen, Q.; Nguyen, T.; Driver, T. G. Iron(II) bromide-catalyzed intramolecular C-H bond amination [1,2]-shift tandem reactions of aryl azides. *J. Am. Chem. Soc.* **2013**, *135* (2), 620−623. (j) Iovan, D. A.; Betley, T. A. Characterization of Iron-Imido Species Relevant for N-Group Transfer Chemistry. *J. Am. Chem. Soc.* **2016**, *138* (6), 1983−1993. (k) Xiong, T.; Zhang, Q. New amination strategies based on nitrogen-centered radical chemistry. *Chem. Soc. Rev.* **2016**, *45* (11), 3069−3087. (l) Park, Y.; Kim, Y.; Chang, S. Transition Metal-Catalyzed C-H Amination: Scope, Mechanism, and Applications. *Chem. Rev.* **2017**, *117* (13), 9247−9301.

(17) Murata, S.; Abe, S.; Tomioka, H. Photochemical Reactions of Mesityl Azide with Tetracyanoethylene: Competitive Trapping of Singlet Nitrene and Didehydroazepine. *J. Org. Chem.* **1997**, *62* (10), 3055−3061.

(18) Arndtsen, B. A.; Sleiman, H. F.; McElwee-White, L.; Rheingold, A. L. Electrophilic reactions of zerovalent tungsten nitrene and hydrazido complexes with phosphines. Synthesis and structure of $(CO)_4W[PPh_2CH_2PPh_2NNMe_2$-N,P]. *Organometallics* **1993**, *12* (7), 2440−2444.

(19) Corona, T.; Ribas, L.; Rovira, M.; Farquhar, E. R.; Ribas, X.; Ray, K.; Company, A. Characterization and Reactivity Studies of a Terminal Copper-Nitrene Species. *Angew. Chem., Int. Ed.* **2016**, *55* (45), 14005−14008.

(20) (a) Jin, L. M.; Lu, H.; Cui, Y.; Lizardi, C. L.; Arzua, T. N.; Wojtas, L.; Cui, X.; Zhang, X. P. Selective Radical Amination of Aldehydic C(sp^2)-H Bonds with Fluoroaryl Azides via Co(II)-Based Metalloradical Catalysis: Synthesis of N-Fluoroaryl Amides from Aldehydes under Neutral and Nonoxidative Conditions. *Chem. Sci.* **2014**, *5* (6), 2422−2427. (b) Roy, S.; Khatua, H.; Das, S. K.; Chattopadhyay, B. Iron(II)-Based Metalloradical Activation: Switch from Traditional Click Chemistry to Denitrogenative Annulation. *Angew. Chem., Int. Ed.* **2019**, *58* (33), 11439−11443. (c) Du, Y. D.; Xu, Z. J.; Zhou, C. Y.; Che, C. M. An Effective [Fe^{III}(TF_4DMAP)Cl] Catalyst for C-H Bond Amination with Aryl and Alkyl Azides. *Org. Lett.* **2019**, *21* (4), 895−899. (d) Kuijpers, P. F.; Tiekink, M. J.; Breukelaar, W. B.; Broere, D. L. J.; van Leest, N. P.; van der Vlugt, J. I.; Reek, J. N. H.; de Bruin, B. Cobalt-Porphyrin-Catalysed Intramolecular Ring-Closing C-H Amination of Aliphatic Azides: A Nitrene-Radical Approach to Saturated Heterocycles. *Chem. - Eur. J.* **2017**, *23* (33), 7945−7952. (e) Gu, Z. Y.; Liu, Y.; Wang, F.; Bao, X. G.; Wang, S. Y.; Ji, S. J. Cobalt(II)-Catalyzed Synthesis of Sulfonyl Guanidines via Nitrene Radical Coupling with Isonitriles: A Combined Experimental and Computational Study. *ACS Catal.* **2017**, *7* (6), 3893−3899.

(21) Wang, H.; Liang, K.; Xiong, W.; Samanta, S.; Li, W.; Lei, A. Electrochemical oxidation-induced etherification via C(sp^3)−H/O−H cross-coupling. *Sci. Adv.* **2020**, *6* (20), No. eaaz0590.

(22) (a) Fiori, K. W.; Du Bois, J. Catalytic intermolecular amination of C-H bonds: method development and mechanistic insights. *J. Am. Chem. Soc.* **2007**, *129* (3), 562−568. (b) Zalatan, D. N.; Du Bois, J. A chiral rhodium carboxamidate catalyst for enantioselective C-H amination. *J. Am. Chem. Soc.* **2008**, *130* (29), 9220−9221. (c) Milczek, E.; Boudet, N.; Blakey, S. Enantioselective C-H amination using cationic ruthenium(II)-pybox catalysts. *Angew. Chem., Int. Ed.* **2008**, *47* (36), 6825−6828.

(23) (a) Wyrzykowski, D.; Kruszyński, R.; Kucharska, U.; Warnke, Z. Structural and Physicochemical Characteristics of Tetrabutylammonium Tetrahalogenoferrates(III), [$(C_4H_9)_4N$][$FeBr_{4-n}Cl_n$]. *Z. Anorg. Allg. Chem.* **2006**, *632* (4), 624−628. (b) Wyrzykowski, D.; Kruszynski, R.; Klak, J.; Mrozinski, J.; Warnke, Z. Magnetic characteristics of Te-trabutylammonium tetrahalogenoferrates(III): X-ray crystal structure of tetrabutylammonium tetrabromoferrate(III). *Z. Anorg. Allg. Chem.* **2007**, *633* (11−12), 2071−2076.

(24) (a) Gill, N. S. 680. Complex halides of the transition metals. Part II. Tetrahedral iron complexes. *J. Chem. Soc.* **1961**, No. 0, 3512−3515. (b) Butcher, K. D.; Didziulis, S. V.; Briat, B.; Solomon, E. I. Variable Photon Energy Photoelectron-Spectroscopy on $FeCl_4^-$: an Unusual Electronic-Structure for High-Spin d^5 Complexes. *J. Am. Chem. Soc.* **1990**, *112* (6), 2231−2242. (c) Feist, M.; Troyanov, S. I.; Mehner, H.; Witke, K.; Kemnitz, E. VII Zwei Oxidationsstufen und vier verschiedene Koordinationen von Eisen in einer Verbindung. Synthese, Kristallstruktur und spektroskopische Charakterisierung von 1,4-Dimethylpiperazinium-Chloroferrat(II, III), ($dmpipzH_2$)$_6$[$Fe^{II}Cl_4$]$_2$[$Fe^{III}Cl_4$]$_2$[$FeIICl_5$] [$Fe^{III}Cl_6$]. *Z. Anorg. Allg. Chem.* **1999**, *625* (1), 141−146. (d) Troyanov, S. I.; Feist, M.; Kemnitz, E. Synthesen und Kristallstrukturen neuer Bromoferrate-(III), Chloro- und Aquachloroferrate(III) mit tetraedrischer und oktaedrischer Eisenkoordination, darunter zwei Neutralkomplexe von Eisen(II) und -(III). *Z. Anorg. Allg. Chem.* **1999**, *625* (5), 806−812. (e) Lauher, J. W.; Ibers, J. A. Structure of tetramethylammonium tetrachloroferrate(II). Comparison of iron(II) and iron(III) bond lengths in high-spin tetrahedral environments. *Inorg. Chem.* **1975**, *14* (2), 348−352. (f) Smith, M. C.; Xiao, Y.; Wang, H.; George, S. J.; Coucouvanis, D.; Koutmos, M.; Sturhahn, W.; Alp, E. E.; Zhao, J.; Cramer, S. P. Normal-mode analysis of $FeCl_4^-$ and $Fe_2S_2Cl_4^{2-}$ via vibrational mossbauer, resonance Raman, and FT-IR spectroscopies. *Inorg. Chem.* **2005**, *44* (16), 5562−5570. (g) Hayashi, T.; Xiao, X.; Fujiwara, H.; Sugimoto, T.; Nakazumi, H.; Noguchi, S.; Fujimoto, T.; Yasuzuka, S.; Yoshino, H.; Murata, K.; Mori, T.; Aruga-Katori, H. A metallic (EDT-DSDTFVSDS)$_2$.$FeBr_4$ salt: antiferromagnetic ordering of d spins of $FeBr_4^-$ ions and anomalous magnetoresistance due to preferential π−d interaction. *J. Am. Chem. Soc.* **2006**, *128* (36), 11746−11747.

(25) Swanson, T. B.; Laurie, V. W. Electron Magnetic Resonance and Electronic Spectra of Tetrachloroferrate(III) Ion in Nonaqueous Solution1. *J. Phys. Chem.* **1965**, *69* (1), 244−250.

(26) Alt, I. T.; Guttroff, C.; Plietker, B. Iron-Catalyzed Intramolecular Aminations of C(sp^3)-H Bonds in Alkylaryl Azides. *Angew. Chem., Int. Ed.* **2017**, *56* (35), 10582−10586.

(27) Bach, R. D.; Wolber, G. J. Theoretical study of the barrier to nitrogen inversion in N-cyano- and N-diazoformimine. Mechanism of the Schmidt reaction. *J. Org. Chem.* **1982**, *47* (2), 239−245.

https://doi.org/10.1021/acscatal.1c00733
ACS Catal. 2021, 11, 7176−7185